Supplementary Information (SI) for Journal of Materials Chemistry A.

Electronic Supplementary Information

Monodisperse fluorinated 3D covalent organic frameworks for enhanced adsorption and extraction of perfluorocarboxylic acids

*Xu-Qin Ran,[b,d] Can Zhu,[b] Qian-Ying Mao,[b] Shu-Ting Xu,[a,b] Shuang-Ping Liu,[a] Peng Gu,[d] Yun Jiang,[d] Xiu-Ping Yan,[a,b,c] and Hai-Long Qian[a,b]**

[a]*State Key Laboratory of Food Science and Resources, Jiangnan University, Wuxi 214122, China.*

[b]*Institute of Analytical Food Safety, School of Food Science and Technology, Jiangnan University, Wuxi 214122, China.*

[c]*Key Laboratory of Synthetic and Biological Colloids, Ministry of Education, School of Chemical and Material Engineering, Jiangnan University, Wuxi 214122, China.*

[d]*Department of Light Chemical Engineering, Jiangnan University, Wuxi 214122, PR China*

Table of Contents

Instrumentation

Scanning electron microscope (SEM) analysis was captured by ZEISS Sigma 360 (Germany). EDS elemental mapping images were obtained by an Oxford Xplore30 (England). X-ray photoelectron spectroscopy (XPS) investigations were executed with an Axis Supra system (Kratos, UK). Powder X-ray diffraction (PXRD) patterns were carried out with a Bruker D2 PHASER instrument (Cu Kα radiation, λ = 1.5418 Å, scanning velocity of 8° min^{-1}, step increment of 0.05° in 2ϑ). Solid-state Fourier transform infrared (FTIR) spectra were conducted on a Nicolet IR IS10 spectrophotometer (USA). Carbon dioxide adsorption-desorption isotherms were measured at 273 K using MicroActive for ASAP 2460 device (USA). Mass spectrometry (MS) was accomplished with an AB SCIEX QTRAP 4500 mass spectrometer (USA) with an AB SCIEX Nanospray II Source (P/N #1004600) and analysis software. Transmission electron microscope (TEM) analysis was captured by JEM-2100PLUS (Japan).

Preparation of monodisperse TAM-TFTA based probe

M-TAM-TFTA based probe was prepared by direct coating method[S1]. A stainless steel needle was immersed in aqua regia (*ca.* 1.5 cm) for 1 min to generate a rough surface, washed with ultrapure water to pH 7.0, and fully dried under nitrogen. The etched needle was then immersed in neutral silica gel sealant dispersed in toluene (*ca.* 1.0 cm), and taken out immediately. Subsequently, the sealant attached needle was rotated in the grinded M-TAM-TFTA powder to form a uniform coating, then washed with ultrapure water and MeOH to obtain M-TAM-TFTA based probe for subsequent extraction experiment.

Adsorption capacity

The adsorption capacity of M-TAM-TFTA or A-TAM-TFTA for PFOA was calculated using the following equation:

$$q_t = \frac{\left(C_0 - C_t\right) \times \mathrm{V}}{\mathrm{m}}$$

In this equation, q_t (mg g^{-1}) is the adsorption capacity of PFOA at t min; C_0 and C_t (mg L^{-1}) are the concentration of PFOA before and after adsorption, respectively; V (L) is the total volume and m (g) is the mass amount of M-TAM-TFTA or A-TAM-TFTA.

Effect of pH on the adsorption

PFOA (400 mg L^{-1}) aqueous solutions at different pH (3-11) were adjust using 0.1 M HCl and 0.1 M NaOH. Then, 1 mg of M-TAM-TFTA or A-TAM-TFTA were mixed in 1 mL PFOA solution at different pH by stirring with 185 rpm at room temperature till equilibrium. Then, the mixture was filtered using 0.22 μm filtration membrane. The collected filtrate was diluted 10,000-fold and the residual PFOA was determined by MS in multiple reaction monitoring (MRM) model with 100 μg L^{-1} of $^{13}C_4$-PFOA as IS.

Adsorption kinetics

1 mg of M-TAM-TFTA or A-TAM-TFTA were mixed in 1 mL PFOA solution (400 mg L^{-1}, pH 5) by stirring with 185 rpm at room temperature for a predetermined time. The mixture was then filtered using 0.22 μm filter membrane. The collected filtrate was diluted 10,000-fold and the residual PFOA was determined by MS in multiple reaction monitoring (MRM) model with 100 μg L^{-1} of $^{13}C_4$-PFOA as IS. The pseudo-first-order kinetic model is calculated as follows:

$$ln(q_e - q_t) = lnq_e - K_1 t$$

The pseudo-second-order kinetic model is calculated as follows:

$$\frac{t}{q_t} = \frac{1}{K_2 {q_e}^2} + \frac{1}{q_e} t$$

where q_e (mg g^{-1}) refers to the adsorption capacity at equilibrium. K_1 (g mg^{-1} min^{-1}) and K_2 (g mg^{-1} min^{-1}) are pseudo-second-order and pseudo-second-order adsorption rate constants, respectively.

Adsorption isotherms

1 mg of M-TAM-TFTA or A-TAM-TFTA were mixed 1 mL PFOA solution (100 - 2000 mg L^{-1}, pH 5) by stirring with 185 rpm at room temperature till equilibrium. The collected filtrate was diluted 10,000-fold and the residual PFOA was determined by MS in multiple reaction monitoring (MRM) model with 100 µg L^{-1} of $^{13}C_4$-PFOA as IS. The Langmuir model equation is given as follows:

$$\frac{C_e}{q_e} = \frac{1}{q_m K_L} + \frac{C_e}{q_m}$$

The Freundlich model equation is given as follows:

$$lnq_e = lnK_F + \frac{1}{n} lnC_e$$

where q_m (mg g^{-1}) is the maximum adsorption capacity, C_e (mg L^{-1}) is the equilibrium concentration of PFOA, K_L (L mg^{-1}) is the Langmuir constant, K_F is Freundlich constant (L min^{-1}), respectively.

Mass transfer resistance

Mass transfer resistance (R_m) is calculated as follows:

$$R_m = \frac{1}{K_2 {q_e}^2}$$

where q_e (mg g^{-1}) refers to the adsorption capacity at equilibrium. K_2 (g mg^{-1} min^{-1}) is pseudo-second-order adsorption rate constants, respectively.

DFT Calculations

DFT theoretical calculations[S3-S7] are executed utilizing the B3LYP method in conjunction with the 6-31G(d) basis set. To further refine our results, we adopted the SCRF (water) method, which comprehensively accounts for the effects of the surrounding solvent environment. The output wavefunction (fchk) files were usedas inputs for Multiwfn to perform the quantitative analysis. The color mappedisosurface graphs of electrostatic potential (ESP) were rendered by

GaussView program. The vdW surface referred throughout this manuscript denotes the iso-surface of r = 0.001 e bohr^{-3}.

Matrix factor

The matrix factor (MF) was calculated by the following equation:

$$MF = \frac{(I_A/I_{IS})_1}{(I_A/I_{IS})_0} \times 100\%$$

where $(I_A/I_{IS})_1$ and $(I_A/I_{IS})_0$ is the ratio of signal intensities for PFCAs and IS in sample matrix and pure water, respectively

Figures of merit

Limit of detection (LOD) and quantification (LOQ) were defined as the concentrations that generating MS peak with signal-to-noise ratio (S/N) value of 3 and 10, respectively. The equations were calculated as follows:

$$LOD = \frac{3S_0}{k}$$

$$LOQ = \frac{10S_0}{k}$$

Where S_0 is the standard deviation of the blank and k is the slope of the linear regression best fit line.

The recoveries for M-TAM-TFTA based PESI-MS analysis of PFCAs in real samples were performed using standard spiking method, and calculated as follows:

$$Recovery = \frac{C_1 - C_2}{C_{Spiked}} \times 100\%$$

Where C_1 is the detected concentration in sample before spiked, C_2 is the detected concentration after spiked, and C_{spiked} is the spiked concentration.

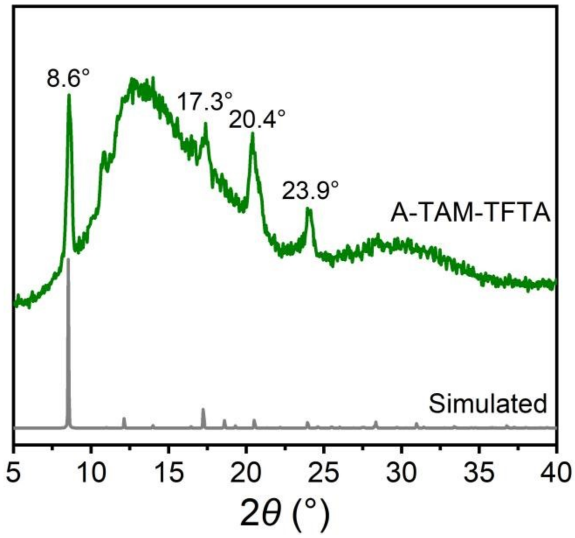

Fig. S1 Experimental and simulated PXRD patterns of A-TAM-TFTA.

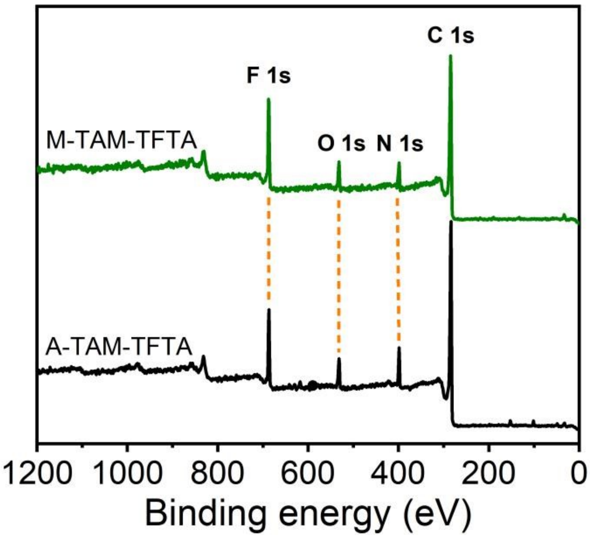

Fig. S2 Wide XPS scanning spectra of M-TAM-TFTA and A-TAM-TFTA.

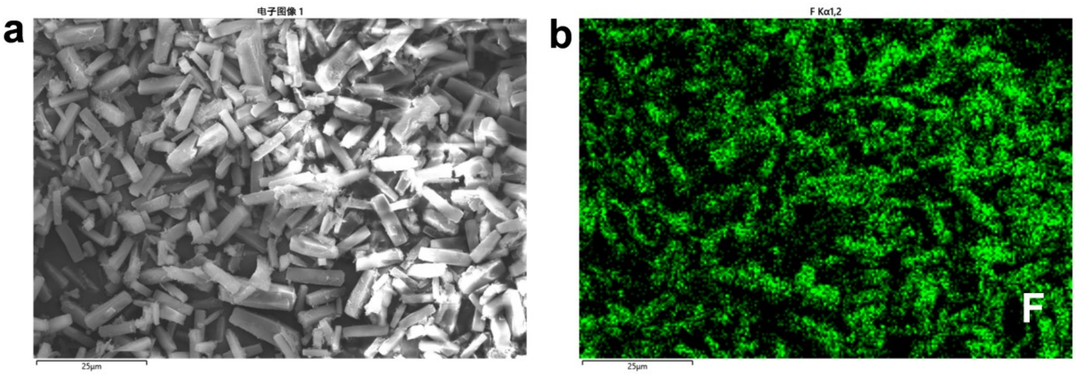

Fig. S3 (a) SEM image and (b) EDS mapping image of M-TAM-TFTA.

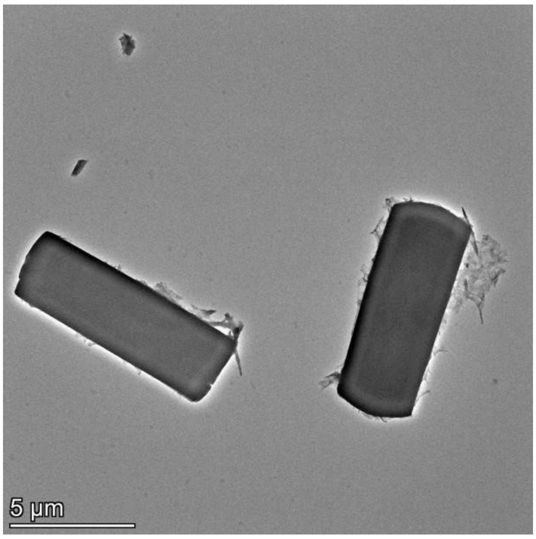

Fig. S4 TEM image of M-TAM-TFTA.

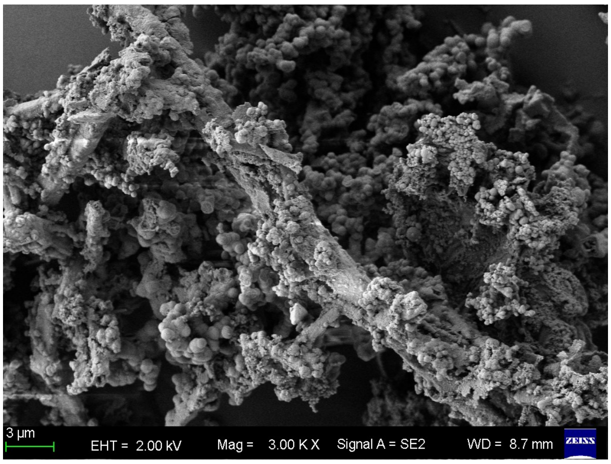

Fig. S5 SEM image of A-TAM-TFTA.

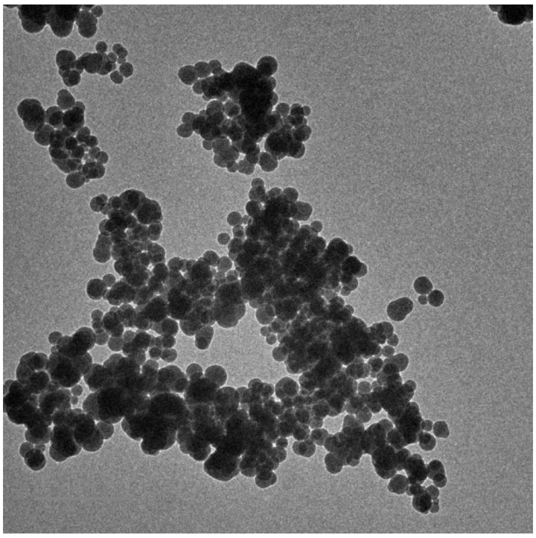

Fig. S6 TEM image of A-TAM-TFTA.

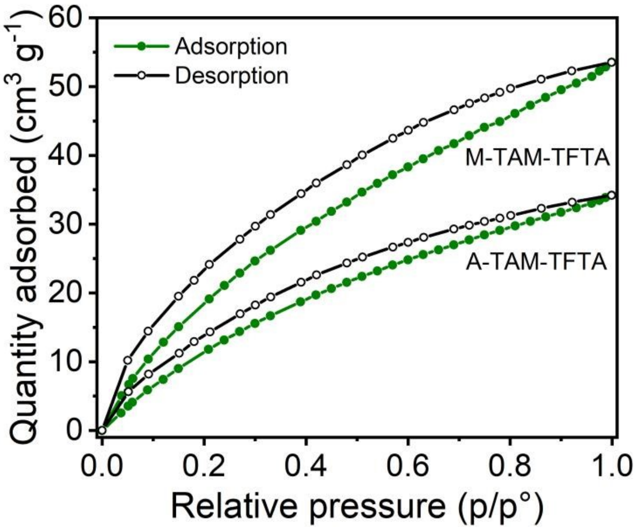

Fig. S7 CO_2 adsorption-desorption isotherms of M-TAM-TFTA and A-TAM-TFTA.

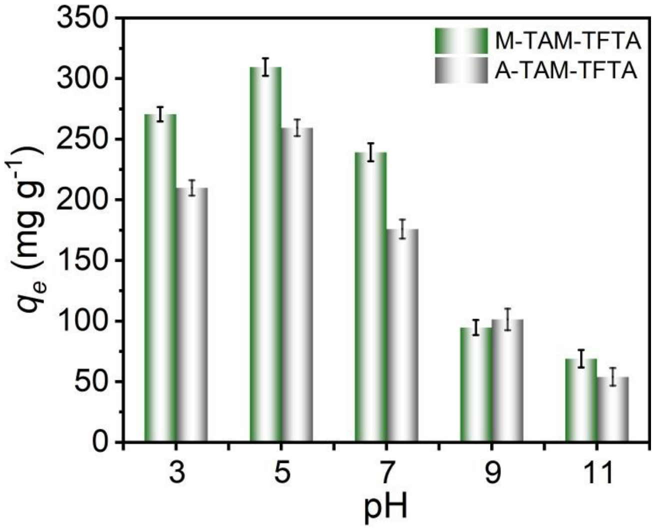

Fig. S8 Effect of pH on PFOA adsorption with M-TAM-TFTA and A-TAM-TFTA.

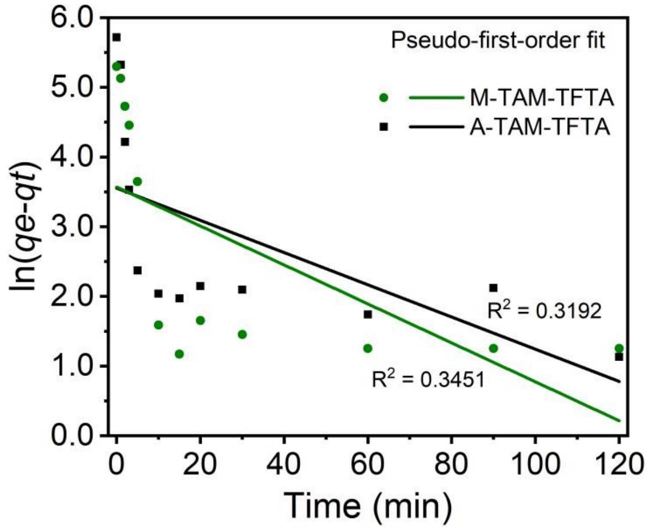

Fig. S9 Pseudo-first order kinetics fitting curves for PFOA adsorption on M-TAM-TFTA and A-TAM-TFTA.

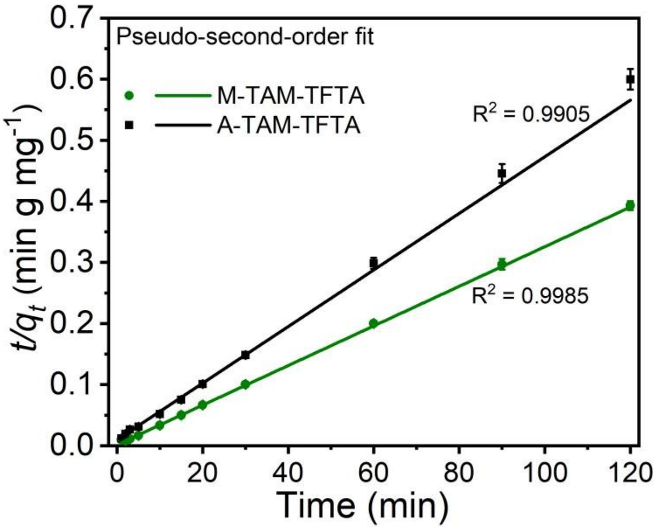

Fig. S10 Pseudo-second order kinetics fitting curves for PFOA adsorption on M-TAM-TFTA and A-TAM-TFTA.

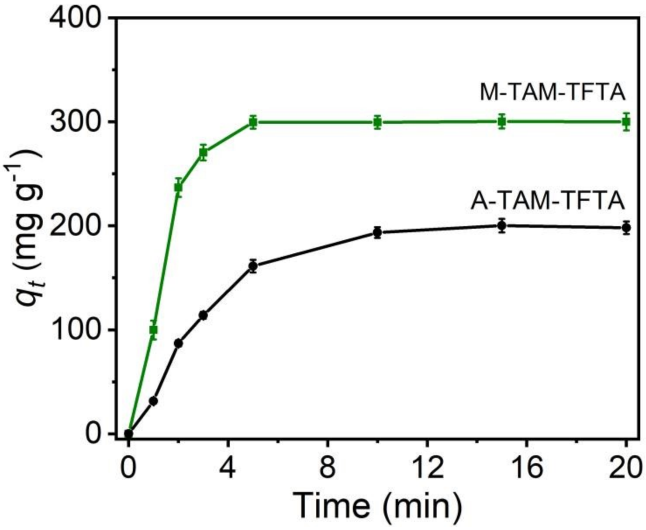

Fig. S11 Effect of time (0-20 min) on PFOA adsorption with M-TAM-TFTA and A-TAM-TFTA.

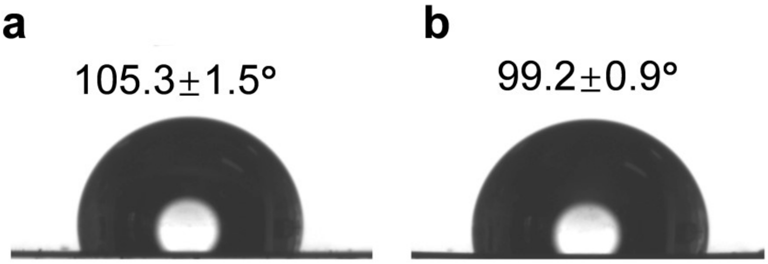

Fig. S12 Water contact angle of (a) M-TAM-TFTA and (b) A-TAM-TFTA.

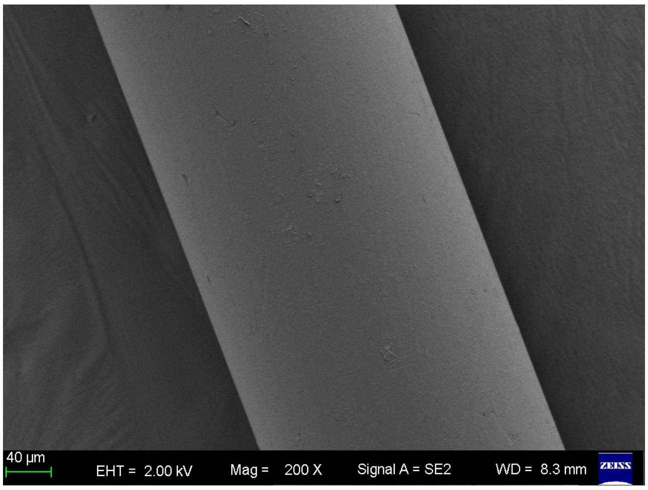

Fig. S13 SEM image of the etched stainless needle.

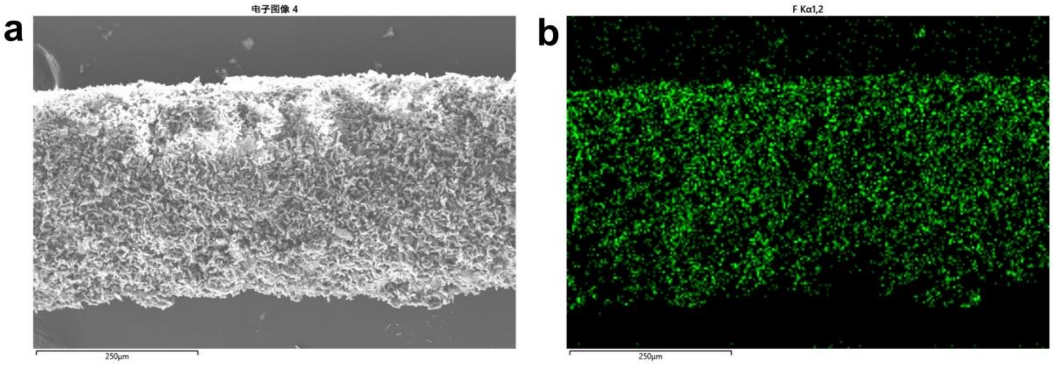

Fig. S14 (a) SEM image and (b) EDS mapping image of M-TAM-TFTA based probe.

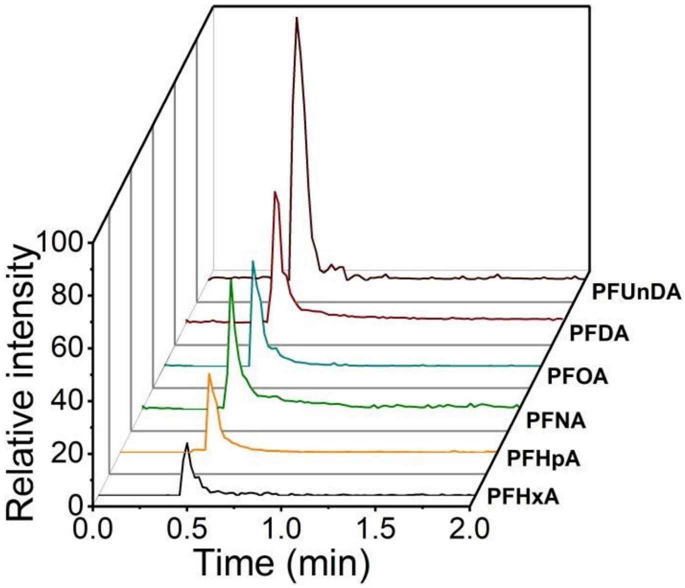

Fig. S15 Elution profile of PFCAs (5000 ng L^{-1}) from M-TAM-TFTA based probe.

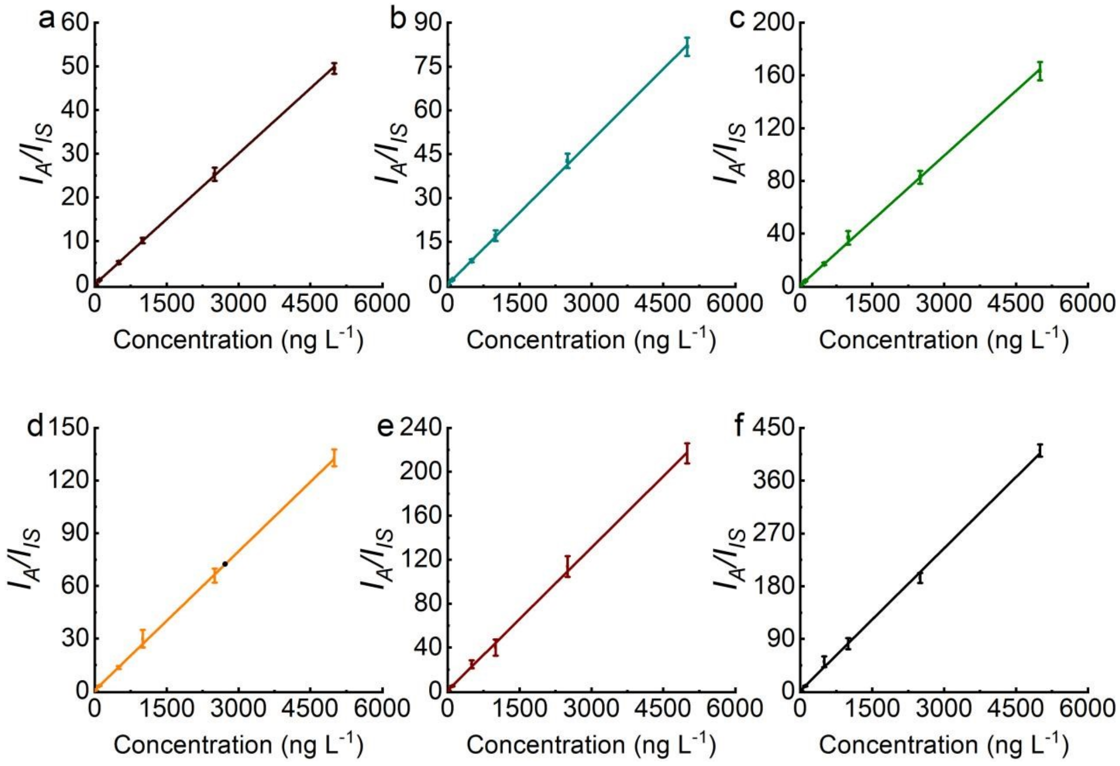

Fig. S16 Calibration curves of (a) PFHxA, (b) PFHpA, (c) PFOA, (d) PFNA, (e) PFDA, (f) PFUnDA with 100 ng L^{-1} of $^{13}C_4$-PFOA as IS. The error bars represent standard deviations of three replicates (n = 3).

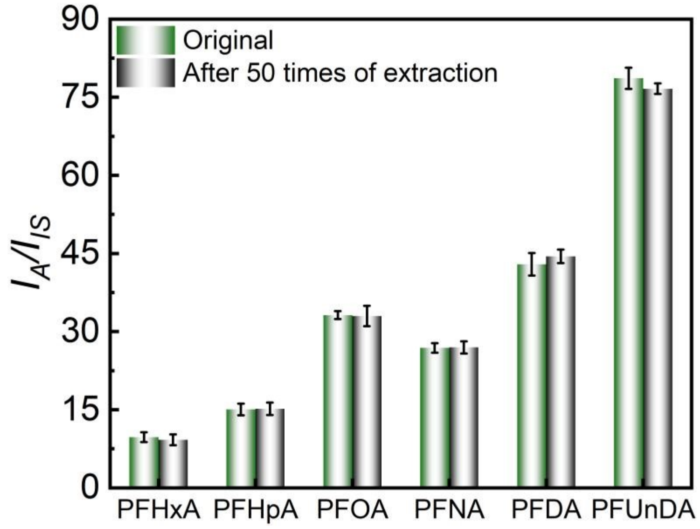

Fig. S17 I_A/I_{IS} of 1000 ng L^{-1} PFOA extracted with the original M-TAM-TFTA based probe and the reused M-TAM-TFTA based probe after 50 extractions.

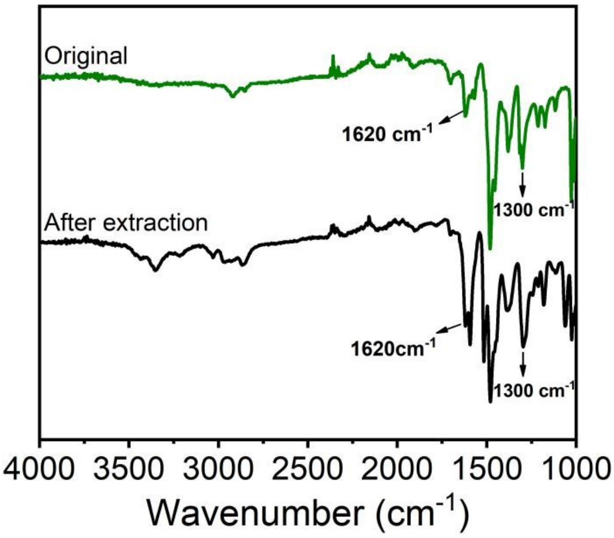

Fig. S18 FTIR spectra of original M-TAM-TFTA and the reused M-TAM-TFTA.

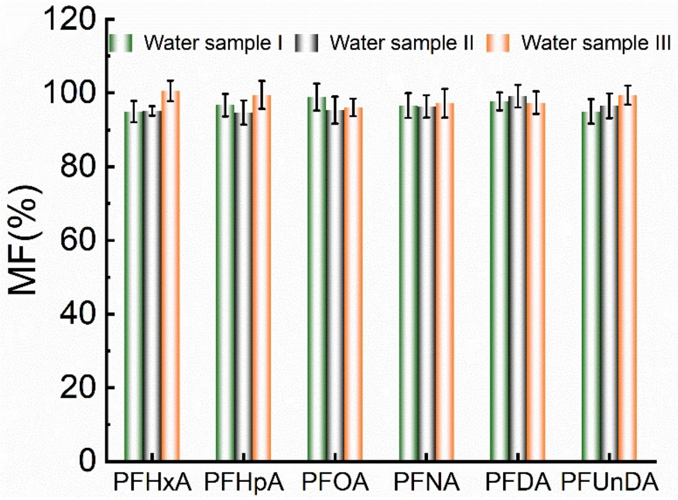

Fig. S19 Matrix factor of water samples on the extraction of PFCAs.

Table S1 Fractional main atomic coordinates for the unit cell of M-TAM-TFTA after pawley refinement.

Space group symmetry *I*41/A
a = b = 20.5537 Å, c = 8.8063 Å, α = β = γ = 90°

Atom	x	y	z
C1	0.49376	0.03772	0.39414
C2	0.53357	0.05208	0.50928
C3	0.5264	0.08876	0.63935
C4	0.47895	0.11255	0.65879
C5	0.43909	0.09844	0.54476
C6	0.4464	0.06157	0.41454
C7	0.47096	0.15131	0.79366
N8	0.50593	0.16445	0.90485
C9	0.4984	0.20442	1.02244
C10	0.5221	0.20235	1.19045
C11	0.51642	0.24156	1.31222
H12	0.57055	0.03281	0.49746
H13	0.55698	0.10013	0.73137
H14	0.40193	0.11734	0.55841
H15	0.41522	0.05158	0.32304
H16	0.4324	0.16904	0.7973
F17	0.54461	0.16834	1.22255
F18	0.53361	0.23876	1.44591
C19	0.5	0	0.25

Table S2 Pseudo-second-order kinetics parameters for PFOA adsorption on M-TAM-TFTA and A-TAM-TFTA

Material	Pseudo-second-order kinetics parameters			
	K_2 (g mg^{-1} min^{-1})	q_e (mg g^{-1})	R^2	R_m (min mg^{-1})
M-TAM-TFTA	0.007	308.6	0.9985	0.0016
A-TAM-TFTA	0.002	216.0	0.9905	0.0107

Table S3 Langmuir and Freundlich parameters for PFOA adsorption on M-TAM-TFTA and A-TAM-TFTA

Material	Langmuir model			Freundlich model		
	q_m (mg g^{-1})	K_L (L mg^{-1})	R^2	n	K_F (L mg^{-1})	R^2
M-TAM-TFTA	554.9	0.009	0.9908	3.38	64.9	0.8363
A-TAM-TFTA	350.8	0.007	0.9845	3.54	43.3	0.83

Table S4 Comparison of reported adsorbents for adsorption of PFCAs.

Analytes	Adsorbent	Adsorption capacity (mg g^{-1})	Ref.
PFOA	Nanoscale zero-valent iron	18	S8
PFOA	Ordered mesoporous carbons	73	S9
PFOA	All-Silica Zeolite Beta	371	S10
PFOA	Zirconium-based metal–organic framework (PCN-1002)	632	S11
PFOA	Zirconium-based metal–organic framework (NU-1000)	507	S12
PFOA	NH_2-functionlized COF	200	S13
PFOS	Fluorinated-squaramide-based COF	375	S14
PFBS	Cationic porous COF	334	S15
PFOA	Monodisperse COF	554.9	This work

Table S5 Multi-reaction monitoring conditions for qualitative and quantitative analysis of PFCAs with PESI-MS.

Analytes	Structure	Parent ion (m/z)	Product ion (m/z)	DP (V)	CE (eV)	EP (V)
PFHxA	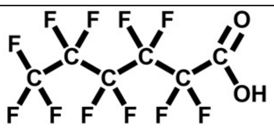	313.1	268.9*	-20	-17	-10
			118.8			
PFHpA	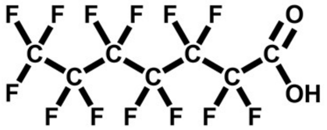	362.8	318.9*	-20	-17	-10
			168.8			
			118.8			
PFOA	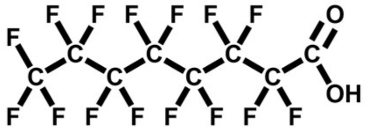	413.0	369.1*	-20	-20	-10
			218.9			
			169.0			
$^{13}C_4$-PFOA (IS)	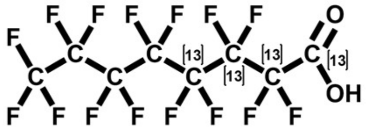	417.0	372.1*	-20	-20	-10
			221.8			
			171.9			
PFNA	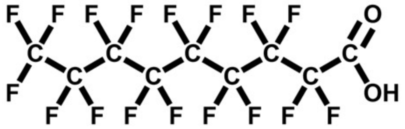	462.5	418.8*	-20	-22	-10
			219.2			
			169.1			
PFDA	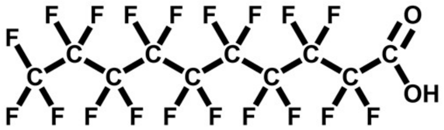	512.7	469.0*	-20	-27	-10
			269.0			
			219.1			
PFUnDa	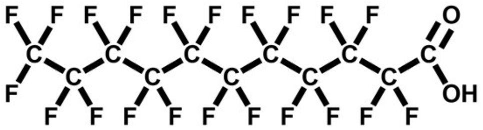	562.7	519.3*	-20	-28	-10
			319.2			
			268.9			

*Ions for quantification

Table S6 Validation of M-TAM-TFTA based PESI-MS for PFCAs

Analytes	Linear range (ng L^{-1})	Regression equation	R^2	LODs (ng L^{-1})	LOQs (ng L^{-1})	Repeatability (RSD, %)	
						One probe	Probe to probe
PFHxA	0.5-5000	Y=0.0101X+0.01842	0.9921	0.14	0.48	3.8	7.9
PFHpA	0.5-5000	Y=0.01641X+0.32971	0.9996	0.26	0.86	4.4	4.8
PFOA	0.5-5000	Y=0.03281X+0.61971	0.9995	0.08	0.27	3.7	8.4
PFNA	0.5-5000	Y=0.02638X+0.42772	0.9996	0.34	1.13	2.5	9.3
PFDA	0.5-5000	Y=0.04335X+0.78402	0.9987	0.46	1.54	6.2	8.9
PFUnDA	0.5-5000	Y=0.08097X+1.60371	0.9983	0.24	0.80	5.3	9.2

Table S7 Comparison of the analytical performances of M-TAM-TFTA based PESI-MS and reported methods for PFCAs.

Method	Adsorbent	LODs (ng L^{-1})	Linear range (ng L^{-1})	Analytical time (min)	Ref.
SPE-GC-MS	Commercial Strata X-AW	0.06 - 14.6	/	＞40	S16
SPE-GC-MS	Molecularly imprinted carbon nanotubes integrating ionic liquids	0.60-1.64	2-100	＞90	S17
GC-MS	/	4-100	100-200000	＞42	S18
SPME-HPLC-MS	Amine and fluorine groups functionalized MIL-101(Cr)	0.004-0.12	0.5-1500	＞15	S19
MSPE/HPLC-MS	Magnetic fluorinated carbon nanotubes	0.010-0.036	0.4-4000	~53	S20
SPE-HPLC- MS	ZIF-67/g-C_3N_4	0.3-2	5-2000	＞30	S21
SPE-HPLC-MS	Chelating resin	10-150	50-5000	30	S22
SPME-AMS	ZIF-8	11	/	~8	S23
SPME-AMS	Reversible F-functionalized COF	0.02-0.8	1-5000	12	S24
SPME-AMS	Monodisperse COF	0.08-0.46	0.5-5000	4	This work

Table S8 Recovery of PFCAs in real sample.

Analytes	Sample	Spiked PFCAs (ng L^{-1})	Determined PFCAs (ng L^{-1}, mean ± s)	Recovery (%) (mean ± s)
PFHxA	Water sample I	0	27.3±3.8	
		100	119.7±7.6	92.5±6.3
	Water sample II	0	10.0±0.8	
		100	101.4±7.9	91.4±8.3
	Water sample III	0	9.4±1.0	
		100	103.1±4.1	93.7±4.8
PFHpA	Water sample I	0	20.0±2.0	
		100	114.1±4.6	93.0±5.8
	Water sample II	0	ND	
		100	99.2±3.1	99.2±3.1
	Water sample III	0	ND	
		100	96.5±3.4	96.5±3.4
PFOA	Water sample I	0	8.0±2.3	
		100	100.0±8.6	91.9±10.8
	Water sample II	0	6.2±0.6	
		100	110.9±1.9	104.7±2.3
	Water sample III	0	2.5±0.8	
		100	95.2±3.0	92.8±3.8
PFNA	Water sample I	0	9.7±1.3	
		100	100.2±7.9	90.5±9.9
	Water sample II	0	15.5±3.8	
		100	110.2±8.0	94.7±5.3
	Water sample III	0	10.0±1.7	
		100	104.7±7.5	94.8±6.3
PFDA	Water sample I	0	28.4±0.8	
		100	121.4±1.8	93.0±4.0
	Water sample II	0	11.8±0.6	
		100	107.9±4.0	96.1±4.1
	Water sample III	0	5.3±1.1	
		100	104.2±4.8	98.9±3.7
PFUnDA	Water sample I	0	ND	
		100	96.6±6.3	96.6±6.3
	Water sample II	0	ND	
		100	99.7±8.7	99.7±8.7
	Water sample III	0	8.8±1.4	
		100	98.3±1.8	89.5±0.5

Reference

(S1) Hou Y. J., Deng J., He K., Chen C., Yang Y. *Anal. Chem.* **2020**, 92, 10213-10217.

(S2) X.-Q. Ran, S.-T. Xu, H.-L. Qian, X.-P. Yan. *J. Hazard. Mater.*, **2023**, 455, 131584.

(S3) Frisch M. J., Trucks G. W., Schlegel H. B., et al. Gaussian 16 Rev. B.01, Wallingford, CT, **2016**.

(S4) Stephens P. J., Devlin F. J., Chabalowski C. F., Frisch M. J. *J. Phys. Chem.* **1994**, 98, 11623-11627.

(S5) Becke A. D. *J. Chem. Phys.* **1993**, 98, 5648-5652.

(S6) Weigend F., Ahlrichs R. *Phys. Chem. Chem. Phys.* **2005**, 7, 3297-3305.

(S7) Weigend F. *Phys. Chem. Chem. Phys.* **2006**, 8, 1057-1065.

(S8) Fang J., Xu K., Liu A., Xue Y., Tie L., Deng Z., Qiu R., Zhang W.-X., *Environ. Sci.: Nano*, **2024,** 11, 1915-1925.

(S9) Lei X., Yao L., Lian Q., Zhang X., Wang T., Holmes W., Ding G., Gang D. D., Zappi M. E., *J. Hazard. Mater.* **2022**, 421, 126810.

(S10) Bergh, M. V., den, Krajnc, A., Voorspoels, S., Tavares, S. R., Mullens, S., Beurroies, I., Maurin, G., Mali, G., DeVos, D. E. *Angew. Chem. Int. Ed.* **2020**, 59, 14086-14090.

(S11) Liang R.-R., Yang Y., Han Z., Bakhmutov V. I., Rushlow J., Fu Y., Wang K.-Y., Zhou H.-C., *Adv. Mater.* **2024**, 36, 2407194.

(S12) Li R., Alomari S., Stanton R., Wasson M. C., Islamoglu T., Farha O. K., Holsen T. M., Thagard S. M., Trivedi D. J., Wriedt M., *Chem. Mater.* **2021**, 33, 3276.

(S13) Ji W., Xiao L., Ling Y., Ching C., Matsumoto M., Bisbey R. P., Helbling D. E., Dichtel W. R., *J. Am. Chem. Soc.* **2018,** *140*, 12677-12681.

(S14) Huang J., Shi Y., Huang G. Z., Huang S., Zheng J., Xu J., Zhu F., Ouyang G. *Angew. Chem. Int. Ed.* **2022**, 61, 202206749.

(S15) Tang S., Qin X., Lv Y., Hu K., Zhao S. *Appl. Surf. Sci.* **2022**, 601, 154224.

(S16) Ye R., Di Lorenzo R. A., Clouthier J. T., Young C. J., VandenBoer T. C., *Anal. Chem.* **2023**, 95, 7648-7655.

(S17) Li G., Cui Y. H., Yang X. N., Xin X. L.,Yan H. Y., Han D. D., *Talanta* **2024**, 275, 126017.

(S18) Ji Y., Cui Z., Li X.; Wang Z., Zhang J., Li A., *J. Chromatogr. A* **2020**, 1622, 461132

(S19) Jia Y., Qian J., Pan B. *Anal. Chem.* **2021**, 93, 11116-11122.

(S20) Huang, Y.; Zhang, W.; Bai, M.; Huang, X., *Chem. Eng. J.* **2020,** *380*, 122392.

(S21) Xie H., Wei Y., Li J., Wang S., Li H., Zhao Y., Zhao M., Chen X. *J. Chromatogr. A* **2020**,1625, 461337.

(S22) Li C. H., Wang Y., Liu J. S, Huang G. L., Zhang B. S., Jiang K. Z. *Anal. Lett.* **2024**, 57, 1515-1525.

(S23) Suwannakot P., Lisi F., Ahmed E., Liang K., Babarao R., Gooding J. J., Donald W. A. *Anal. Chem.* **2020**, 92 , 6900-6908.

(S24) Hou Y. J., Deng J., He K., Chen C., Yang Y. *Anal. Chem.* **2020**, 92, 10213, 10217.